Available online at www.sciencedirect.com
SCIENCE DIRECT®
Analytica Chimica Acta 518 (2004) 93–100
ANALYTICA CHIMICA ACTA
www.elsevier.com/locate/aca

The dynamic response of optical oxygen sensors and voltammetric electrodes to temporal changes in dissolved oxygen concentrations

Brian T. Glazer, Adam G. Marsh*, Kevin Stierhoff, George W. Luther, III

Graduate College of Marine Studies, University of Delaware, Lewes, DE 19958, USA

Received 16 January 2004; received in revised form 17 May 2004; accepted 17 May 2004

Abstract

Accurately measuring dissolved oxygen concentrations in fresh and salt water environments has long been an interdisciplinary priority. Many methodologies exist, including two very promising new ones, optical fluorescence quenching optrodes (or optodes) and solid-state voltammetric electrodes. In this study we compare the responsiveness of these two techniques to dynamic changes in dissolved oxygen concentrations, using traditional methods of polarographic oxygen sensors and Winkler's chemical titrations to corroborate the measurements. Advantages of the optrode system include simplicity of operation and high sensitivity when changes in oxygen concentrations are small ($<\Delta 10\,\mu M\,O_2\,min^{-1}$). Advantages of voltammetry include equally high sensitivity, independent of rate of change of oxygen concentration, and the capability of simultaneously measuring other chemical species. Both systems have the capability of producing high-resolution, continuous oxygen profiles by collecting and reporting real-time data. Kinetic estimates of the binding and dissociation constants for the ruthenium–oxygen complex in the optrode revealed a relatively long half-life of the Ru^{2+}–O_2 complex for dissociation ($t_{1/2}$ of 43.2 s to equilibrate from a 100 to 0% O_2 saturation change). In contrast, the Ru^{2+}–O_2 association constant was 5.0 times faster ($t_{1/2}$ of 8.6 s to equilibrate from a 0 to 100% O_2 saturation change). Therefore, because of these differential kinetics, researchers should take care when using a ruthenium-based optrode to measure real-time dissolved oxygen concentrations undergoing temporal variability.

Keywords: Oxygen sensors; Electrodes optrodes; Optodes; Dissolved oxygen; Voltammetry

1. Introduction:

The reduction of oxygen to water (aerobic respiration) and the converse oxidation of water to oxygen (oxygenic photosynthesis) are two of the most fundamental biological redox reactions in our biosphere (Eqs. (1) and (2)).

$$O_2 + 4H^+ + 4e^- \rightarrow 2H_2O \quad (1)$$

$$2H_2O \rightarrow 4H^+ + 4e^- + O_2 \quad (2)$$

In all marine environments there is a boundary transition from oxic to anoxic conditions, driven by the decomposition of organic matter exhausting the supply of available oxygen. Subsequent organic oxidation reactions require alternate oxidants from the manganese, nitrogen, iron, and sulfur systems. Such a boundary can occur at or below the sediment–water interface [1,2], or in the case of heavily eutrophied or stratified systems, higher in the water column [3–5]. Accompanying the transition from oxic to anoxic (or sulfidic) waters are steep gradients of various oxidants and reductants, making precise measurements of low concentrations of oxygen (and other constituents) particularly desirable in biogeochemical studies. The importance of measuring concentrations of dimolecular oxygen (O_2) also crosses broad biological disciplines, from ecosystem structure to cellular function.

Consequently, the marine sciences have a long history of developing techniques for measuring dissolved oxygen concentrations: redox chemical titrations [6], Cartesian divers [7–9], polarographic oxygen sensors [10,11], coulometric capacitance respirometers [12–14], couloximetric respirometers [15,16], solid-state voltammetric electrodes [17,18] and optical fluorescence quenching [optodes or optrodes [19–22]].

* Corresponding author. Tel.: +1-3026454367.
E-mail address: amarsh@udel.edu (A.G. Marsh).

0003-2670/$ – see front matter © 2004 Published by Elsevier B.V.
doi:10.1016/j.aca.2004.05.040

New technological approaches to measuring dissolved oxygen concentrations have been developed because of a combination of needs: increasing sensitivity [12], decreasing sample volumes (<100 μl) [23], and reducing the technical expertise necessary to make measurements [21,22]. Two recently developed methodologies (optrodes and solid-state voltammetry) have received considerable interest in marine science because of the micro-scale measurements they are capable of making. Optrodes are promising because of their simple operation and high sensitivity. Voltammetry is promising because of high sensitivity and flexibility in simultaneously measuring other ionic species in solution. Both systems are advantageous because of their ability to make real-time, continuous measurements, in small volumes, without measurement-induced consumption of oxygen confounding their accuracy or precision. Thus both systems are very attractive because of the potential for making measurements under dynamic conditions, yet no studies have actually been conducted to compare or calibrate the dynamic responsiveness of either methodology. In this study we compare the temporal responsiveness of optrodes and voltammetric electrodes while performing controlled changes in the dissolved oxygen concentrations in seawater and freshwater.

2. Materials and procedures

2.1. Optical fluorescent probes

Several methodologies have been developed for the optical detection of O_2, however, the most commonly employed strategy depends on the quenching response of an oxygen sensitive fluorophore, such as transition–metal organic complexes [24]. In general, electrons can be excited in the metal–organic complex at a specific wavelength of light (λ_{ex}), and once the excitation energy in those electrons is released, the complex will emit light at a different wavelength (λ_{em}, simple fluorescence). However, these fluorophore compounds are also reactive with oxygen, which will bind the transition metal moiety and block (quench) the fluorescence activity of the compound [20,25]. The amount of inhibition or quenching is directly proportional to the concentration of oxygen surrounding the compound and thus, quantifying the inhibition of fluorescence is used in optrode systems to optically measure oxygen concentrations in solution [26,27].

In this study, a commercially available optrode has been used (Ocean Optics, single-channel FOXY system, Boca Raton, FL, USA). The optrode detector consisted of a 1 mm diameter optical fiber cable encased in a stainless-steel tube with a ruthenium (Ru^{2+}) organic complex coated on the detection window of the fiber, and protected by another, silicon coating. A pulsed blue LED light source (LS-450) provided an excitation wavelength of 470 nm, a scanning spectrophotometer (USB2000) monitored the full-spectrum light emission (400–800 nm), and a USB interface between the spectrophotometer and a computer allowed the emission maxima (597 nm) to be continuously monitored using the manufacturer's software (OOIFOXY). Two-point calibration concentrations using 0% (N_2 purged) and 100% (aerated) O_2 saturated seawater or freshwater were used to calibrate the fluorescent quenching response of the optrode using the manufacturer's recommended procedures and software. At all times, temperatures of the reference and experimental samples were kept constant by using circulating water baths with antagonistic heaters and chillers. This optrode system has been successfully used for measuring oxygen consumption rates in the zoeal larval stages of the Asian shore crab, *Hemigrapsus sanguineus* [21]. All methodologies used in any one experiment were calibrated simultaneously using the same standard solutions.

2.2. Solid-state voltammetric electrodes

With the solid-state gold/amalgam (Au/Hg) microelectrode, oxygen, sulfur species, iodide, Fe(II), Fe(III), Mn(II), and FeS can all be simultaneously measured [1,17,28] because each redox species, if present, produces a current peak that can be discriminated from others in one potential scan from −0.1 to −2.0 V (analogous to varying wavelength and measuring absorbance with UV-Vis spectroscopy). Furthermore, since the voltammetric electrode scans a range of potentials, rather than constantly resting at a single potential, consumption of the ion species measured is undetectable.

Briefly, a standard three-electrode cell was used in all electrochemical measurements. The potentiostat used was a portable Analytical Instruments Systems, Incorporated (AIS, Inc.) DLK 100a electrochemical analyzer. The working electrode was a gold amalgam (Au/Hg) electrode of 0.1 mm diameter, sealed with epoxy into commercially available polyethyletherketone (PEEK^{TM}) tubing [17,18]. Counter (Pt) and reference (Ag/AgCl) electrodes, each of 0.5 mm diameters, were also made in PEEK^{TM} tubing. Linear sweep voltammetry (LSV) was employed, scanning from −0.1 to −2.0 V at a scan rate of 1000 mV s^{-1}, although scan rates of up to 5000 mV s^{-1} have been successfully employed to further reduce time required for data acquisition. Electrochemically conditioning the electrode between scans removed any chemical species from the surface of the electrode, restoring it for the next measurement. Electrodes were calibrated in 0% (N_2 purged) and 100% (air-saturated) O_2 saturated seawater (or freshwater, depending on experiment) prior to experiments, and repolished, replated, and re-calibrated if sensitivity was lost. The detection limit is about 3 μM for O_2.

The Advanced Analysis software package (AIS, Inc.) was used for manually analyzing peak heights of individual voltammograms that are generated during data acquisition. In order to provide rapid analysis of continuous measurements over long periods of time (generating thousands of voltammograms), a software application was written to provide automatic analyses of peak heights and positions

for the direct calculation of O_2 concentrations (ScanVolt 1.0: C++, Win2000 OS, with full GUI support). The application's output was repeatedly checked against manual peak height measurements throughout the experiments. Over 4400 voltammetric scans were analyzed for the data presented in Figs. 2–4.

2.3. Corroborative measurements

In addition to the continuous measurements using optrode and voltammetric electrode sensors, oxygen was periodically measured using Winkler titrations, and a Yellow Springs Instruments (YSI) Model 5100 bench top dissolved oxygen meter equipped with a YSI Model 5010 self-stirring Clark-type polarographic (amperometric) membrane electrode. The YSI meter and probe were calibrated to 0% (N_2 purged) and 100% (fully aerated) saturation according to manufacturer's specifications. The YSI system automatically compensates for changes in temperature, giving it a potential advantage over other methods in field applications. Winkler titrations followed the protocol of the Chesapeake Bay Institute [29], incorporating dispensettes for reagent addition, and a Metrohm autotitrator (model 716 DMS Titrino) for titration.

2.4. Calibration protocol

Instrument calibration is of particular importance for measuring dissolved oxygen because standard additions or multi-point calibration curves are currently problematic. All measurements were performed at sea level, so no atmospheric pressure corrections were needed. Furthermore, constant temperature was maintained and salinity was measured before and after experiments to ensure no evaporation took place. We followed the air-saturated water calibration guideline established by the USGS [30]. Briefly, water of the same temperature and salinity as the targeted sample was aerated with an electric pump and gas diffusion stone for 5–10 min. For 100% saturation, theoretical oxygen saturation was calculated based on temperature and salinity [31] and assigned to the current maximum for the electrode, and the fluorescence-quenching maximum for the optrode. The same solution was then purged of oxygen using argon or nitrogen gas through the diffuser. Zero percent oxygen saturation was assumed when no detectable current was present for the electrode and fluorescence was 100% for the optrode. Optrode, voltammetric electrode, and YSI membrane electrode were simultaneously calibrated in the same solutions, which were also assayed directly with Winkler titrations.

2.5. Experimental control of dissolved O_2 concentrations

Dissolved oxygen concentrations were manipulated by one of two methods for the following experiments. For discrete measurements and calibrations, an aquarium air pump

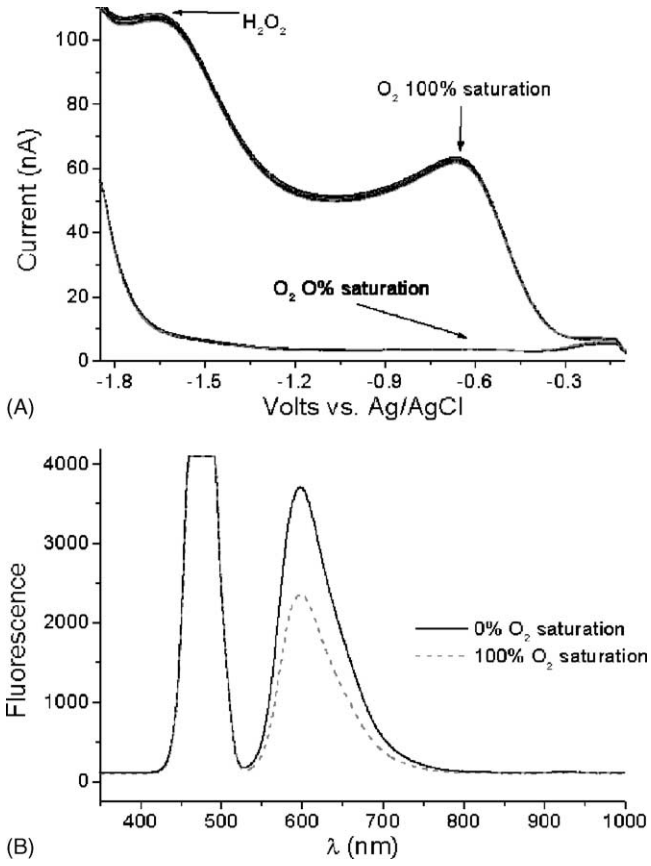

Fig. 1. (a) Representative voltammograms of O_2 calibration in seawater. Electrochemical reduction of oxygen to peroxide at the electrode surface is measurable as the peak at −0.65 V (E_p). The current peak (difference between current at −0.2 and −0.65 V = 56 nA) is proportional to the concentration of dissolved oxygen in the sample ($n = 8$). The voltage at the half-height is called $E_{1/2}$. The peak at −1.67 V represents the reduction of the newly formed peroxide at the electrode surface to water, and is equal to the signal for oxygen if no ambient peroxide is present (difference between current at −1.0 and −1.67 V = 56 nA). In environments such as biofilms and microbial mats, an excess of peroxide has been observed, indicating a background concentration of peroxide in the environment [34]. After 10 min of purging the sample with N_2 or Ar gas, the peaks are not visible, indicating no oxygen was present ($n = 4$, MDL = 3 μM). (b) Calibration of the optrode plot of excitation and emission for the ruthenium dye complex. The optrode surface is excited by exposure to 470 nm light with a corresponding fluorescence at ∼600 nm that is quantitatively proportional to the presence of oxygen associated with the Ru^{2+}-fluorophore.

was utilized to achieve 100% saturation, and argon or nitrogen gas was used to achieve decreases in oxygen concentration (Figs. 1A,B and 2). To achieve a slow, defined rate of change in dissolved oxygen concentrations over longer periods of time a computer-controlled recirculating sea water system was used [32], employing a negative-feedback design, where oxygen concentration was regulated in response to deviations from a user-defined setting. The system consisted of a PC running a LabVIEW™ virtual instrument (LabVIEW™, National Instruments Corp.) interfaced with a microcathode, polarographic oxygen electrode coupled to an analog Strathkelvin Model 781 oxygen meter and a re-

circulating aquarium system equipped with compressed O_2 and N_2 sparging lines in the head tanks. This system has the capacity to regulate oxygen at constant or cycling levels for indefinite periods of time. Adjustments to the system were made at ~2 min intervals to maintain tight control over desired profiles of changing oxygen concentrations. The oxygen concentration in the head reservoir was increased or decreased as necessary through the addition of compressed O_2 or N_2, respectively. Thus, oxygen concentration in the experimental container was indirectly regulated by the flow of oxygenated or de-oxygenated water from the head tank. This method of adjustment minimized rapid fluctuations in ambient oxygen concentration that are ordinarily introduced by the direct addition of compressed gas to an experimental container.

3. Assessment

Both voltammetry and optical fluorescence methodologies produce a dynamic output response that covers a spectrum of energies: electron reduction potentials and visible light spectrum, respectively. In the representative calibration voltammograms (Fig. 1A), a peak in current (nA) occurs on the voltage ramp at the potential specific for the redox species of interest (Eqs. (3) and (4)). For O_2, E_p and $E_{1/2}$ can shift more negatively with increasing scan rate (1000 mV/s throughout this study).

$$O_2 + 2H^+ + 2e^- \rightarrow H_2O_2,$$
$$E_p = -0.65\,V, \quad E_{1/2} = -0.49\,V \tag{3}$$

$$H_2O_2 + 2H^+ + 2e^- \rightarrow 2H_2O,$$
$$E_p = -1.67\,V, \quad E_{1/2} = -1.44\,V \tag{4}$$

The magnitude of the current peak is directly proportional to the molar concentration of these molecules in solution [33]. Note the reproducibility of the several repetitive scans for both 0 and 100% O_2 saturation. In the case of optical fluorescence (Fig. 1B), peaks in the emission light spectrum associated with Ru^{2+} fluorescence are quantitatively related to the molar concentration of O_2 in solution [25]. A clear advantage to interpreting the output response of these two techniques is that they provide a spectrum or data profile for analysis. A simple visual inspection of the profile is often sufficient to ensure the quality of the data being collected during an experiment.

The first critical assessment of the dynamic response of both sensor technologies was to determine the stability of their measurements over long periods of time (48 h). Both detection methodologies are completely solid-state and the stability of the signal output evidences no appreciable sensor drift even following rapid changes in O_2 concentrations (between 0 and 100% saturation over 4 h; Fig. 2). However, the two sensors show an intriguing difference in the response profiles to these large changes in O_2 concentrations. When

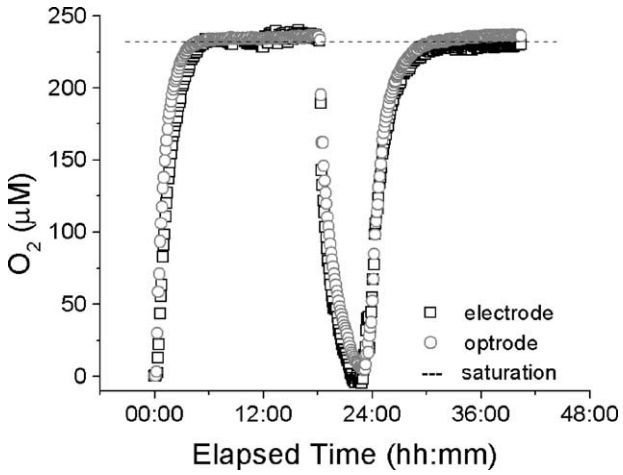

Fig. 2. Forty hours of continuous measurements by the electrode and optrode in the same seawater sample. Temperature was maintained at 20 °C and salinity was 34, making 100% saturation 231 μM O_2. Electrode and optrode measurements were synchronized and taken every 13 min. Dissolved oxygen concentration was lowered by purging a headspace with N_2, or opening the headspace to the atmosphere, allowing for O_2 diffusion back into solution.

O_2 is rapidly increasing, the optrode signal appears to lead the electrode signal in terms of responding to the increase in availability of O_2. Conversely, when O_2 is rapidly declining, the electrode signal appears to lead the optrode signal in responding to a lower availability of O_2. Although both systems reflect high stability and equivalent stable measurements, they appear to have different dynamic characteristics associated with how they respond to changes in O_2 concentrations.

Using a controlled O_2 gradient, we were able to characterize the dynamic response of these sensors with greater resolution in terms of their O_2 sensitivities, cycling between 50 and 100% saturation over 6 h (Fig. 3). A slower rate

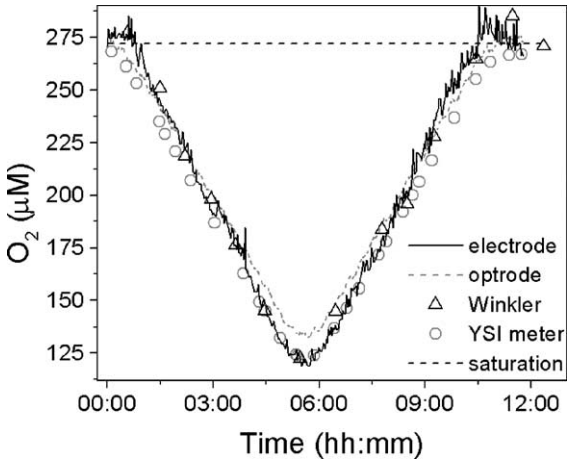

Fig. 3. Twelve hours of continuous measurements by the electrode and optrode, with frequent Winkler and YSI sampling. Temperature was maintained at 22 °C and salinity was 0, making 100% saturation 272 μM O_2. Dissolved oxygen concentration was manipulated by a feedback-controlled solenoid system controlling the mixing of N_2 and O_2 gas inputs.

of change in O_2 concentrations resulted in a closer signal profile between the electrode and optrode. However, at O_2 concentrations below 75% saturation, the O_2 concentration measured by the optrode was consistently higher than the concentration measured by the electrode. In this experiment, corroborative measurements using both direct Winkler titrations and YSI oxygen-probe measurements indicated that the electrode values were consistently equivalent to these other measurement techniques while the optrode measurements were consistently higher when O_2 levels were below 75% sat. Overall, there is an apparent reduction in the measurement accuracy of the optrode system when O_2 concentrations are changing, even over gradual gradient profiles.

It is interesting to note that the YSI oxygen-probe measurements were lower than all three other methods when O_2 saturation was between 75 and 100%. It is possible that the high O_2 consumption rate of this probe confounds its measurements (even with active stirring).

Rapid cycling of O_2 tensions between 60 and 80% saturation (every 30 min) was used to quantify the dynamic response of the techniques and to assess the sensitivity of the optrode to variable O_2 concentrations (Fig. 4). Corroborative measurements of O_2 concentrations were also made with the YSI oxygen probe. The rapidity of the O_2 cycling that was maintained in the experimental system was too quick for the optrode to reach an accurate equilibrium with the surrounding water. During the experimental time course, optrode measurements were always higher than the corresponding electrode and YSI measurements.

The optrode measurements in Figs. 2 and 3 show a slight delay in reaching an equilibrated reading (relative to the other methods); however, this inaccuracy was accentuated when O_2 concentrations were rapidly cycled (Fig. 4). The optrode response suggests a non-linear interaction between the Ru^{2+}-fluorophore and the availability of O_2 such that when O_2 concentrations are declining, the Ru^{2+}-fluorophore does not release its bound oxygen proportionally to the rate at which the external oxygen concentration is decreasing. Thus, there is an apparent 'lag' in the optrode response indicating that more time is necessary for the oxygen bound by the Ru^{2+} to come to equilibrium with the surrounding water. Conversely, when O_2 concentrations are increasing, the Ru^{2+}-fluorophore binds proportionally more oxygen than the rate of increase in oxygen availability. Although this results in an apparent 'rapid' response of the optrode to increasing O_2, the optrode measurements are too high in comparison to the electrode and YSI measurements.

First-order decay constants [k in $f(e^{-kt})$] were estimated using the full "approach to equilibrium" data to characterize the formation and dissociation of the Ru^{2+}–O_2 binding complex when the optrode was exposed to 0% (Ar gassing) and 100% (air gassing) saturated distilled water (no ions to confound the Ru^{2+} and O_2 interaction). The decay constant for formation ($\sim k_f$) was 4.82 min^{-1} ($\pm$0.03S.E., $n = 7$, $r^2 = 0.982$; Fig. 5) and the decay constant of dissociation ($\sim k_d$) was 0.96 min^{-1} ($\pm$0.01S.E., $n = 7$, $r^2 = 0.964$; Fig. 6). Overall, these decay constants indicate that the Ru^{2+}–organic complex has a 5.0-fold greater affinity (ratio k_f:k_d) for binding oxygen than for releasing it once it is bound. The dissociation decay constant can be used to estimate the half-life of the Ru^{2+}–O_2 binding complex when oxygen is removed from the system. This value ($t_{1/2}$) was 43.2 s indicating a relatively slow equilibration period for this process. In contrast, the half-life of the unbound Ru^{2+}-fluorophore (at 0% saturation) was only 8.6 s when the optrode was exposed to 100% saturated water. It is intrigu-

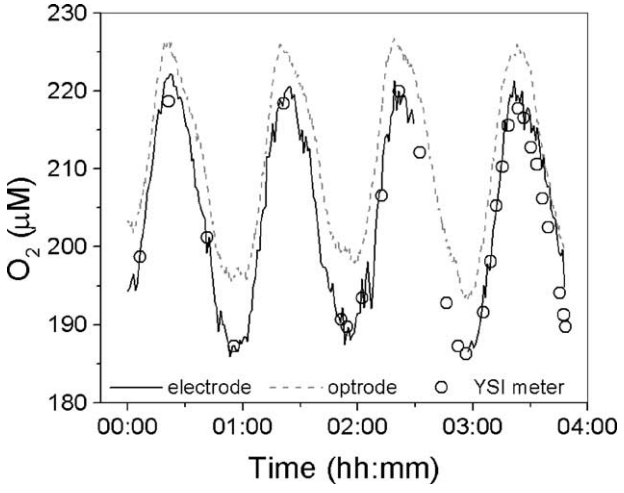

Fig. 4. Four hours of continuous measurements by the electrode and optrode, with frequent YSI sampling. Temperature was maintained at 22 °C and salinity was 0, making 100% saturation 272 μM. The break in the electrode measurements (2:30–3:00 h) was due to a sequence error in the continuous data collection software. It is noteworthy that the optrode deviates from the electrode by roughly 50% more at lower concentrations than at higher concentrations.

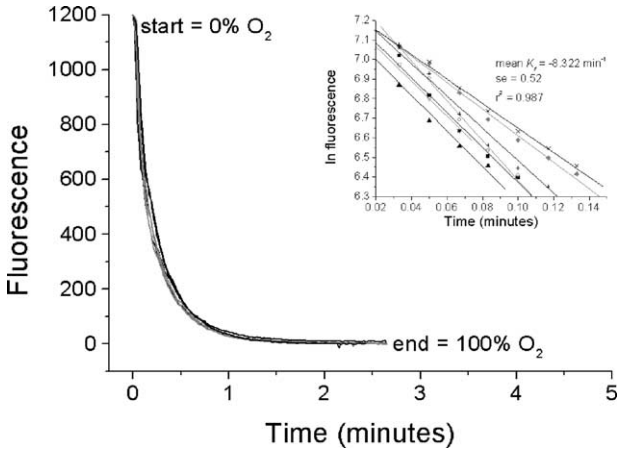

Fig. 5. Pseudo first-order binding kinetics for the formation of the Ru^{2+}–O_2 complex. Fluorescence intensity over time following the transfer of the optrode between 0 and 100% O_2 saturated water used the following model: rate of formation (loss of fluorescence) $y = a e^{-kt}$, where $-k = k_f$. The model yielded a decay constant of 4.82 min^{-1} and $t_{1/2} = 8.6$ s. Initial rate theory revealed first-order kinetics (inset), yielding a rate constant of 8.32 min^{-1} and $t_{1/2} = 5$ s.

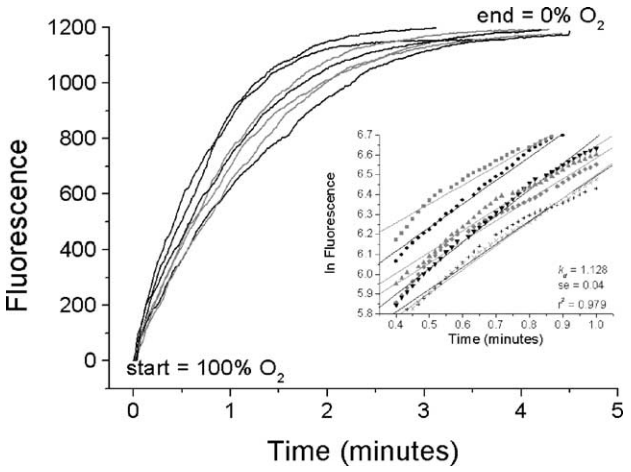

Fig. 6. Dissociation shows mixed zeroth-order and first-order kinetics. Fluorescence intensity over time following the transfer of the optrode between 100 and 0% O_2 saturated water used the following model: rate of formation (loss of fluorescence) $y = a(1 - e^{-kt})$, where $-k = k_d$. The model yielded a decay constant of $0.96\,min^{-1}$ and $t_{1/2} = 43.2\,s$. The initial 0.4 s of the reaction displayed zeroth-order kinetics ($r^2 = 0.978$) followed by pseudo first order kinetics through 1 s ($k_d = 1.12\,min^{-1}$, $t_{1/2} = 36.9\,s$).

ing to note the consistent response profile that was obtained when the optrode was transferred from 0 to 100% O_2 saturated water (Fig. 5), in contrast to the level of variation in the profiles obtained when the optrode was transferred from 100 to 0% O_2 saturated water (Fig. 6). This difference most likely results from micro-scale diffusion gradients that are setup when the Ru^{2+}–O_2 complex is dissociating and the unbound Ru^{2+} will repeatedly re-bind an O_2 molecule until the O_2 has diffusively moved away from the surface of the optrode, even though vigorous turbulence from the gas bubbling enhanced diffusion from the optrode surface in these experiments. The Ru^{2+}-fluorophore's 5.0-fold greater affinity for O_2 likely produces a series of 're-binding' events that are numerous and stochastic to produce the observed variance in profiles (Fig. 6).

In addition, we have estimated a pseudo, first-order kinetic constant for the Ru^{2+}–O_2 formation using initial rate theory to evaluate the kinetics of the interaction during the first 0.15 s of the reaction (from 0 to 60% of complete binding; Fig. 5 inset). The k_f estimated by a linear regression of ln(fluorescence) against time was $8.32\,min^{-1}$ (±0.52S.E., $n = 7$, $r^2 = 0.987$, $t_{1/2} = 5\,s$). This indicates that for the optrode tested (with a protective silicon over-coating) the initial binding interaction is psuedo first-order, after which the interaction is determined by an approach to equilibrium, which could be confounded by diffusion processes associated with the silicon over-coating of the optrode used. The kinetic constant for the dissociation of the Ru^{2+}–O_2 interaction is more complex to assess (Fig. 6 inset). The initial 0.4 s (36% dissociation) of the reaction appears to display zeroth-order kinetics (data not shown, $r^2 = 0.978$), while the period from 0.4 to 1 s (36–76% dissociation) evidences first-order kinetics ($k_d = 1.12\,min^{-1}$, ±0.04S.E., $n = 7$, $r^2 = 0.979$, $t_{1/2} = 36.9\,s$). Application of these first-order kinetic constants yields an equilibrium constant ($K = k_f/k_d$) of 7.4, which is nearly 50% greater than the ratio of the decay constants determined above (5.0). This difference most likely results from the calculation of the decay constants that includes the period of an approach to equilibrium. The kinetic constants give a more precise idea of the interaction rate between Ru^{2+} and O_2, however, in practice, the simple decay constants are more straightforward to calculate and provide useful information regarding the kinetic performance of an optrode system.

4. Discussion

When the oxygen concentration was below 225 μM O_2 (75% saturation), the differences in measured oxygen concentrations were the greatest between the optrode and electrode (Fig. 3, *t*-test, $P < 0.001$). This implies that the electrode measurements display a more rapid response to a sudden change in oxygen availability, while the optrode measurements reflect the time-dependency required for reaching equilibration. The key observation is that on a time scale of minutes the optrode response displays a chemical behavior that favors the retention of oxygen by the Ru^{2+}-flurophore. Overall, the oxygen measurements of these two methods do not respond equivalently to rapid ($>\Delta 10\,\mu M\,O_2\,min^{-1}$) changes in oxygen concentrations, with the optrode measurements exhibiting a response lag that is dependent upon the absolute concentration of oxygen present. Apparently the molecular mechanism of the Ru^{2+}–O_2 interaction does not result in a linearly proportional change in Ru^{2+}–O_2 binding in response to rapid changes in O_2 availability.

The key to interpreting the different dynamic response profiles of the optrode and electrode systems lies in considering the molecular mechanism of the signal produced in the presence of oxygen. The electrode system is straightforward, as an applied potential at the electrode surface results in a peak in current that is proportional to the concentration of the molecule in the solution. The more oxygen present, the greater the energy flux (Fig. 1A). In contrast, the optrode provides an indirect measurement by assessing the binding kinetics between a Ru^{2+}-fluorophore and O_2 by quantifying the resulting decrease in fluorescence. The more oxygen present, the more the fluorescence will be quenched and hence the smaller the response signal will be (Fig. 1B). Thus the two biggest differences between these methodologies are: (1) the measured responses are inverse such that at high O_2 concentrations the electrode gives high signal output while the optrode gives a low signal output, and (2) the reaction at the electrode surface is a direct one, involving only oxygen and its electrochemical reduction while the optrode requires a binding equilibrium to be established between the Ru^{2+}-fluorophore and oxygen in order for the fluorescence inhibition measurements to be quantitative.

Therefore, the binding kinetics of the Ru^{2+} for oxygen are likely to produce the apparent discrepancies in optrode measurements when oxygen concentrations are changing over short time intervals (30 min). If for any single optrode the actual molecular interaction between the Ru^{2+}-fluorophore and molecular oxygen can be described as a simple first-order interaction, then the reaction can be described by just two rate constants governing their association and dissociation:

$$\text{Rate of formation} = k_f[Ru^{2+}][O_2] \quad (5)$$

$$\text{Rate of dissociation} = k_d[Ru^{2+}\text{–}O_2 \text{ complex}] \quad (6)$$

$$\text{Apparent affinity constant} = K = \frac{k_f}{k_d} \quad (7)$$

If $k_f = k_d$, then the Ru^{2+}-fluorophore will both bind and release oxygen directly proportional to the concentration of oxygen in the external medium. In this scenario, the Ru^{2+}-fluorophore would evidence an almost instantaneous equilibration between its associated O_2 and the dissociated O_2 surrounding it. However, if $k_f > k_d$, then the binding function would favor the retention of O_2 associated with the Ru^{2+}-fluorophore and this would introduce a time-lag necessary for the amount of O_2 associated with the Ru^{2+}-fluorophore to reach an equilibrium with the surrounding O_2 concentration. This is the case for the dynamic response profiles of the optrode in Figs. 2–4, where $k_f > k_d$. Here, at any given concentration of O_2, a greater proportion of the Ru^{2+}-fluorophores are more likely to be associated with an O_2 molecule than without one. As O_2 concentrations decrease, the instantaneous differences between the proportions of associated versus dissociated Ru^{2+}–O_2 will increase, resulting in a greater discrepancy of the immediate optrode signal response relative to the actual O_2 concentrations. Even when time between measurements was 13 min (Fig. 2) the optrode seemed to lag, suggesting that dissociation is hindered. A possible explanation accounting for this is that the protective silicon coating over the Ru^{2+}-fluorophore is acting to retain or retard O_2 diffusion away from the reactive surface of the optrode.

From the controlled O_2 profiles in this study, we can estimate that changes in O_2 concentrations in excess of $\Delta 10\,\mu M\ O_2\,min^{-1}$ are too rapid for a binding equilibrium to be established at the surface of the optrode (0.78 mm^2 surface-response area). However, if the optrode is exposed to lower rates of change in O_2, the period of disequilibrium becomes less noticeable and hence, less of a confounding factor impacting the optrode response. It is important to note that the comparisons pursued in this study were designed to determine the performance limits for either the electrode or optrode in terms of their dynamic response profiles. Both the optrode and electrode systems are highly accurate for stable oxygen concentrations as demonstrated by the number of publications that have successfully employed these methodologies, and as shown in Fig. 2.

However, the optrode system is rapidly gaining favor in the marine sciences because of its combined ease of operation and accuracy [13,19,20,22]. Despite the wealth of calibration data using optrodes to demonstrate their efficacy for direct measurements of oxygen concentrations, this study represents the first critical evaluation of the dynamic response of the optrode measurements to temporal changes in oxygen concentrations. As more researchers look to using optrodes for dynamic profiling (real-time respiration rates, water-column oxygen gradients, sediment oxic–anoxic transitions), there needs to be a greater emphasis placed on understanding the temporal dynamics of the Ru^{2+}–O_2 binding kinetics in order to ensure that oxygen concentration measurements are accurate. Following first-order kinetics indicates that the system is directly responding to the concentration of oxygen of the system. Following zeroth-order kinetics implicates adsorption dynamics, possibly attributable to confounding dissolution through a protective silicon overcoating (Atkins 1982).

5. Comments and recommendations

1. Both the optrode and electrode systems offer highly accurate measurements of oxygen concentrations in a real-time, continuous monitoring profile. The advantage of the optrode is that the system is technically simple to operate and maintain. (Typical costs are as follows: Ocean Optics optrode, light source, and scanning spectrophotometer, US$4500; AIS DLK100a electrochemical analyzer, electrochemical cell stand, counter, reference, working electrodes, US$8,000. In addition, each system also requires a computer interface for instrument control and data acquisition.) The advantage to the electrode system is that the measurements are direct, non-selective, and responsive to rapid changes in concentrations.
2. When using optrode systems, the absolute rate of change in external oxygen concentrations should be kept as minimal as possible. For example, when profiling O_2 in a water column, great care should be exercised in maintaining a slow descent rate through a gradient. Moving through an oxygen pycnocline would require several minutes for equilibration of the Ru^{2+}–O_2 complex, as greater than $\Delta 10\,\mu M\ O_2\,min^{-1}$ would confound the depth location and resolution of that gradient. Water column profiles using the electrode system are not confounded by moderate descent rates since scan rate can be increased to provide for less than 2 s of data acquisition per scan. Therefore voltammetric methods are more reliable than Ru^{2+}-based optrodes for producing high-resolution vertical profiles of oxygen gradients across an oxic–anoxic transition zone.
3. Researchers measuring respiration rates through continuous monitoring (rather than end-point sampling) should be aware of the binding kinetics of Ru^{2+} and O_2, which will vary with the concentration of Ru^{2+} on the optrode

and the surface area of the optical fiber. The apparent dependency on external oxygen concentrations for optrode equilibration means that estimates of oxygen binding and dissociation rates should be corrected (cross-calibrated) for the absolute changes in oxygen concentrations. The inclusion of at least the first-order decay constants for an optrode used in any publication would be useful for assessing the performance of that system.

4. Further studies should target methods to calibrate real-time oxygen detection instruments using controlled rates of change in oxygen concentrations rather than static calibration points. The recirculating system used in this study is one example of control through mechanical manipulation. If a defined chemical reaction could be initiated to produce a quantitative rate of oxygen removal from a system, then real-time monitoring devices could be calibrated to that exact rate of chemical oxygen consumption, as well.

Acknowledgements

We gratefully acknowledge the assistance of S. Curless in running the Winkler titrations, T. Szela for assistance with optrode calibrations, and Dr. T. Targett for providing the controlled oxygen recirculating water system. This research was supported by grants from the National Science Foundation to AGM (OCE-0095459) and GWL (OCE-0096365 and OCE-0308398) and the NOAA Sea Grant program to GWL (NA16RG0162-03).

References

[1] G.W. Luther III, P.J. Brendel, B.L. Lewis, B. Sundby, L. Lefrancois, N. Silverberg, D.B. Nuzzio, Limnol. Oceanogr. 43 (1998) 325.
[2] M. Taillefert, T.F. Rozan, B.T. Glazer, J. Herszage, R.E. Trouwborst, G.W. Luther III, in: M. Taillefert, T.F. Rozan (Eds.), Environmental Electrochemistry: Analyses of Trace Element Biogeochemistry, vol. 811, American Chemical Society, Washington, DC, 2002.
[3] L.G. Anderson, D. Dyrssen, P.O.J. Hall, Mar. Chem. 23 (1988) 283.
[4] M.I. Scranton, Y. Astor, R. Bohrer, T.-Y. Ho, F. Muller-Karger, Deep Sea Res. Part I: Oceanogr. Res. Pap. 48 (2001) 1605.
[5] J.W. Murray, L.A. Codispoti, G.E. Friederich, in: C.P. Huang, C.R. O'Melia, J.J. Morgan (Eds.), Aquatic Chemistry: Interfacial and Interspecies Processes, vol. 244, American Chemical Society, 1995, 157 pp.
[6] L.W. Winkler, Chemische Berichte 21 (1888) 2843.
[7] J. Gray, Biol. Rev. 1 (1925) 227.
[8] J. Lang, Biologisches Zentralblatt 54 (1934) 85.
[9] E. Zeuthen, Compte rendu des travaux du Laboratoire de Carlsberg, Ser. Chim. 24 (1943) 479.
[10] J.S. Kahn, Anal. Chem. 9 (1964) 389.
[11] L.C.J. Clark, Trans. Am. Soc. Artif. Int. Org. 2 (1956) 41.
[12] A.A. Huesner, J.P. Hurley, R. Arbogast, Am. J. Physiol. 243 (1982) R185.
[13] A.G. Marsh, D.T. Manahan, Mar. Ecol. Progr. Ser. 184 (1999) 1.
[14] O. Hoegh-Guldberg, D.T. Manahan, J. Exp. Biol. 198 (1995) 19.
[15] L.S. Peck, M.J. Whitehouse, J. Exp. Mar. Biol. Ecol. 163 (1992) 163.
[16] L.S. Peck, E. Prothero-Thomas, Mar. Biol. 141 (2002) 271.
[17] P.J. Brendel, G.W. Luther III, Environ. Sci. Technol. 29 (1995) 751.
[18] G.W. Luther III, C.E. Reimers, D.B. Nuzzio, D. Lovalvo, Environ. Sci. Technol. 33 (1999) 4352.
[19] I. Klimant, F. Ruckruh, G. Liebsch, C. Stangelmayer, O.S. Wolfbeis, Mikrochim. Acta 131 (1999) 35.
[20] M.D. Stokes, G.N. Somero, Limnol. Oceanogr. 44 (1999) 189.
[21] A.G. Marsh, S. Cohen, C.E. Epifanio, Mar. Ecol. Progr. Ser. 218 (2001) 303.
[22] S. Gatti, T. Brey, W.E.G. Muller, O. Heilmayer, G. Holst, Mar. Biol. (Berlin), Online 19 February 2002.
[23] L.S. Peck, R.F. Uglow, J. Exp. Mar. Biol. Ecol. 141 (1990) 53.
[24] J.R. Bacon, J.N. Demas, Anal. Chem. 59 (1987) 2780.
[25] I. Klimant, V. Meyer, M. Kuhl, Limnol. Oceanogr. 40 (1995) 1159.
[26] B. Meier, T. Werner, I. Klimant, O.S. Wolfbeis, Sens. Actuat. B: Chem. 29 (1995) 240.
[27] I. Klimant, P. Belser, O.S. Wolfbeis, Talanta 41 (1994) 985.
[28] S.M. Theberge, G.W. Luther III, Aq. Geochem. 3 (1997) 191.
[29] J.H. Carpenter, Limnol. Oceanogr. 10 (1965) 141.
[30] D.B. Radtke, A.F. White, J.V. Davis, F.D. Wilde, in: F.D. Wilde, D.B. Radtke (Eds.), National Field Manual for the Collection of Water-Quality Data, vol. 9, US Geological Survey Techniques of Water-Resources Investigations, USGS Information Services, Denver, CO, USA, 1998, Chapter A6.2. http://water.usgs.gov/owq/FieldManual/Chapter6/Section6.2.pdf
[31] R.F. Weiss, Deep Sea Res. 20 (1970) 291.
[32] P.A. Grecay, K.L. Stierhoff, J. Exp. Mar. Biol. Ecol. 280 (2002) 53.
[33] D.A. Skoog, D.M. West, Fundamentals of Analytical Chemistry, 3rd ed., Holt, Rinehart, and Winston, New York, NY, USA, 1976.
[34] B.T. Glazer, S.C. Cary, L. Hohmann, G.W. Luther III, in: M. Taillefert, T.F. Rozan (Eds.), Environmental Electrochemistry: Analyses of Trace Element Biogeochemistry, vol. 811, American Chemical Society, Washington, DC, 2002.